Transport and thermal properties of weakly ferromagnetic Sr_2IrO_4

2006 J. Phys.: Condens. Matter 18 8205

(http://iopscience.iop.org/0953-8984/18/35/008)

INSTITUTE OF PHYSICS PUBLISHING JOURNAL OF PHYSICS: CONDENSED MATTER

J. Phys.: Condens. Matter **18** (2006) 8205–8216 doi:10.1088/0953-8984/18/35/008

Transport and thermal properties of weakly ferromagnetic Sr_2IrO_4

N S Kini[1,2], A M Strydom[3], H S Jeevan[1], C Geibel[1] and S Ramakrishnan[4]

[1] Max-Planck Institute for Chemical Physics of Solids, Noethnitzer Strasse 40, Dresden D-01187, Germany
[2] Department of Applied Chemistry, Graduate School of Engineering, Hiroshima University, Higashi, Hiroshima 739-8527, Japan
[3] Physics Department, University of Johannesburg, PO Box 524, Auckland Park 2006, South Africa
[4] Department of Condensed Matter Physics, Tata Institute of Fundamental Research, Mumbai-400 005, India

E-mail: kini@hiroshima-u.ac.jp

Received 13 March 2006, in final form 12 July 2006
Published 15 August 2006
Online at stacks.iop.org/JPhysCM/18/8205

Abstract

We have synthesized polycrystalline Sr_2IrO_4 and measured its magnetic susceptibility, electrical resistivity, specific heat, Seebeck coefficient, and thermal conductivity. The magnetic susceptibility $\chi(T)$ shows a ferromagnetic transition at 250 K while the behaviour above the transition temperature is well described by a Curie–Weiss fit with a small effective moment $\mu_{\rm eff} = 0.33\ \mu_{\rm B}$ and a paramagnetic Curie–Weiss temperature, $\theta_{\rm CW} = +251$ K, consistent with previous studies on this compound. However, specific heat, Seebeck coefficient, and thermal conductivity are all dominated by the phonon contribution and show no anomalies at the ferromagnetic transition. Electrical resistivity, unlike the single crystal, shows a huge increase, three orders of magnitude, with decreasing temperature. The temperature dependence of resistivity is logarithmic at high temperatures (210 K $< T <$ 350 K), Arrhenius type in intermediate temperatures (110 K $< T <$ 190 K) with a small energy gap of $\Delta = 37$ meV, and variable-range-hopping type at low temperatures (35 K $< T <$ 80 K), in contrast to the data reported for single crystals. These results can be understood if localized states are present near the Fermi level due to structural oxygen disorder in this low dimensional compound.

1. Introduction

Iridates such as $BaIrO_3$ [1], Sr_2IrO_4 [2], and $Sr_3Ir_2O_7$ [3], in which the Ir ion is in the 4+ state, have been known to show weak ferromagnetism with relatively high transition temperatures (T_c) and very small effective moment values ($\mu_{\rm eff}$), significantly smaller than the free-ion

moment expected for an $S = 1/2$ spin. They have also been reported to show unusual electrical properties, with overall semiconducting behaviour. For example, in $BaIrO_3$ the onset of a weak ferromagnetic transition coincides with that of a charge density wave (CDW) formation [1]. Strontium iridates such as Sr_2IrO_4 [2] and $Sr_3Ir_2O_7$ [3] show weak ferromagnetism with small values of μ_{eff} and a overall semiconductor-like electrical conductivity.

In these oxides, the Ir^{4+} ion is sixfold coordinated with oxide ions to form IrO_6 octahedra. In a regular octahedral environment, the oxide-ion crystal field splits the d orbitals of the Ir^{4+} ion into two sets of degenerate orbitals, namely two e_g orbitals with slightly higher energy than three t_{2g} orbitals. Due to elongation of the Ir–O bonds (2.058 Å) along one of the crystallographic axes, the degeneracy in the t_{2g} orbitals is lifted, and the $5d^5$ electrons of the Ir^{4+} ion will occupy a low spin-1/2 state with one unpaired electron. While the free-ion moment expected for Ir^{4+} in the low spin state amounts to $\mu_{eff} = 1.73\ \mu_B$, all these compounds show $\mu_{eff} \ll 1.73\ \mu_B$ and a very small saturation moment, μ_s. Since applied magnetic fields as high as even 55 T have not been able to bring about any metamagnetic or spin–flop transition in these compounds [1, 3], and the observed effective moment in the paramagnetic region is very small, a local moment scenario of ferrimagnetism or canted antiferromagnetism does not appear to be valid for these compounds. The weak itinerant magnetism of the Ir ion at high temperatures in these compounds basically comes from the small net moment due to spin polarization which arises because of the difference in the occupation of majority (up) and minority (down) spin states of t_{2g}-block bands [4]. This is also consistent with the Stoner criteria (enhancement of susceptibility with no concomitant increase in γ, the heat capacity coefficient). Such a Stoner enhancement is possible in these systems due to the presence of localized states at the Fermi level due to structural disorder as observed in the recent photoemission studies of $BaIrO_3$ [5].

In the case of Sr_2IrO_4, all previous investigations focussed on the structural (neutron and x-ray), magnetic and transport (resistivity) properties. No attempt was made to understand its thermal properties. For instance, single crystal studies on Sr_2IrO_4 showed a ferromagnetic transition at $T_c = 240$ K with a small μ_{eff} and μ_s [2]. The resistivity was anisotropic with an overall semiconductor-like behaviour. Earlier investigations on polycrystalline samples reported them to be insulating [6–8]. But for a preliminary report of resistivity between 150 and 300 K [9], no temperature-dependent resistivities were reported for polycrystalline samples. However, the magnetic properties were similar to those of single crystals. In order to throw more light on the nature of spin and charge correlation in this compound, we prepared good quality single phase polycrystalline Sr_2IrO_4 and measured its magnetic, electrical transport, thermopower, thermal conductivity and specific heat data. While our magnetic data are consistent with those reported for single crystals, the transport and thermal data can be construed to suggest a gapped system with the presence of localized states near the band edge.

2. Experimental procedure

Single-phase polycrystalline Sr_2IrO_4 samples were prepared by the reaction of $SrCO_3$ with high purity Ir metal powder in air for 24 h at 1273 K with intermediate grindings. For the purpose of physical measurements, bulk specimens were prepared by pelletizing the Sr_2IrO_4 powder and sintering the same at 1273 K for 24 h in flowing oxygen to ensure that the oxidation is complete. Thermogravimetry in flowing argon up to 1273 K on the powder of the sintered pellets showed that the loss of mass at the highest temperature is less than 1%, indicating that the oxygen is quite stable in this compound.

X-ray diffraction data obtained from the powder of the sintered pellets confirmed the formation of a single-phase compound with the refined tetragonal lattice parameters $a =$

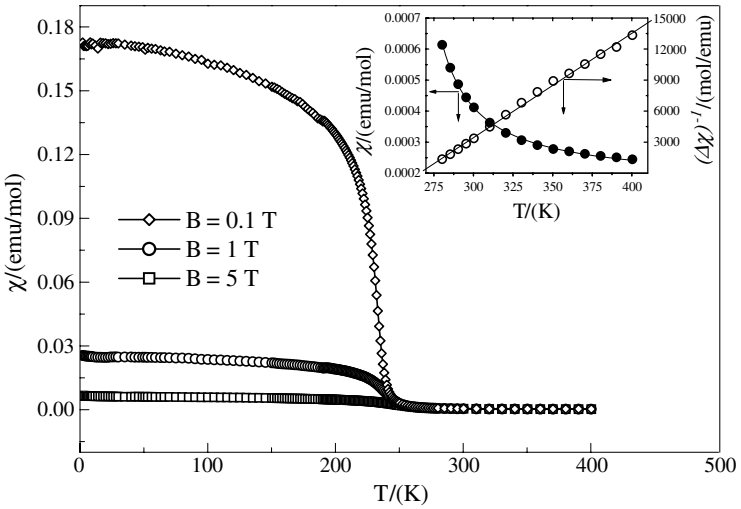

Figure 1. Temperature dependence of the magnetic susceptibility, $\chi(T)$, of Sr_2IrO_4. The inset shows $\chi(T)$ in the paramagnetic region, measured in 5 T along with a plot of $(\Delta\chi)^{-1}$ versus T where $\Delta\chi = \chi - \chi_0$ (see text).

5.496(1) Å, and $c = 25.774(1)$ Å (space group *I41/acd*) in excellent agreement with the reported values of both polycrystalline [6, 7, 10] and single-crystalline data [2].

Magnetic properties were measured using a Quantum Design (QD) magnetic property measurement system (MPMS) in the temperature range 2–400 K with a maximum field of 5 T. The specific heat was measured between 2 and 290 K by the heat pulse relaxation method using a QD physical property measurement system (PPMS). The Seebeck coefficient (S) and thermal conductivity (κ) were measured on a QD PPMS using the thermal transport option (TTO). Resistivity was measured by the standard four-probe technique by the AC-transport method on a QD PPMS. Previous studies [2] on single crystals reported a non-Ohmic behaviour in Sr_2IrO_4, and therefore we have intentionally made use of a very small excitation current (I) of 10 μA between 60 and 350 K, and $I < 10$ μA for $T < 60$ K. No hysteresis was observed during heating–cooling cycles in any of our measurements.

3. Results and discussion

3.1. Magnetic susceptibility

Figure 1 shows the temperature dependent magnetic susceptibility $\chi(T)$, measured under the field cooled (FC) condition, in applied fields of $B = 0.1$, 1, and 5 T. A sharp ferromagnetic transition at 250 K is evident from the figure. The magnetic susceptibility at $T = 0$ K (extrapolated from the $\chi(T)$ versus T plot for $B = 1$ T) is 0.025 emu mol^{-1}, which is in good agreement with comparable data reported previously for polycrystalline Sr_2IrO_4 (0.022 emu mol^{-1}) [6]. The averaged value of χ of single-crystal data using the equation $\chi_{av} = (2\chi_{\|a} + \chi_{\|c})/3$ (measured in 0.5 T) is 0.11 emu mol^{-1}, which is in good agreement with our value for 0.5 T measurements, 0.10 emu mol^{-1}.

The saturation moment μ_s, obtained by extrapolating the high-field part (4 T $< B <$ 5 T) of the M versus B straight line (obtained at $T = 2$ K) to zero, amounts to $\mu_s = 0.045$ μ_B/Ir. We have also estimated the μ_s value of the polycrystalline sample from the previously

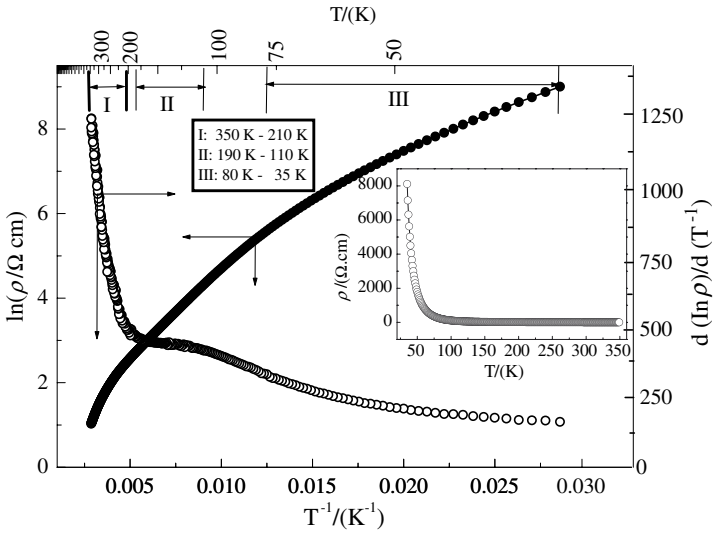

Figure 2. Plot of $\ln \rho$ versus T^{-1} (closed circles) and its differential $\mathrm{d}(\ln \rho)/\mathrm{d}(T^{-1})$ versus T^{-1} (open circles) for Sr_2IrO_4. The inset shows the temperature dependence of resistivity.

reported [6] magnetization data (obtained at $T = 5$ K) to be roughly 0.03 μ_B/Ir [6], clearly indicating better quality of our samples. However, the single-crystal-averaged value of magnetization $(2M_{\|a} + M_{\|c})/3 = 0.11$ μ_B/Ir [2] is significantly higher than our value.

Above the transition temperature T_c, the susceptibility $\chi(T)$ follows a modified Curie–Weiss law given by equation (1):

$$\chi(T) = \chi_0 + \frac{C}{T - \theta_{CW}} \tag{1}$$

where $C = N_A \mu_{eff}^2/3k_B$ is the Curie constant, μ_{eff} is the effective magnetic moment, θ_{CW} is the paramagnetic Curie–Weiss temperature and χ_0 is a small temperature-independent susceptibility. The values obtained from the fit were $\theta_{CW} = +251$ K, $\mu_{eff} = 0.33$ μ_B/Ir and $\chi_0 = 1.5 \times 10^{-4}$ emu mol^{-1} (using 1 T data, fitting between 270 and 400 K).

Although the value of θ_{CW} agrees very well with the reported single-crystal value of +251 K [2], μ_{eff} is slightly smaller and χ_0 is much smaller than the values reported for a single crystal, 0.5 μ_B/Ir and 8.8×10^{-4} emu mol^{-1} respectively [2]. Since the ferromagnetism in Sr_2IrO_4 is very weak as well as anisotropic, some variation in the results of magnetization measurements is not uncommon. It is of interest to note that the magnetic susceptibility data of polycrystalline samples used for neutron diffraction could not be fitted with a Curie–Weiss model above T_c [6], which shows clearly that our polycrystalline samples are of better quality.

3.2. Resistivity measurements

The temperature dependence of the resistivity, $\rho(T)$, is shown in the inset of figure 2. The room-temperature resistivity of our polycrystalline sample is about 4 Ω cm, which is of the same order of magnitude as that reported for a single crystal of Sr_2IrO_4 [2]. Below room temperature, the sample shows an overall semiconductor-like behaviour consistent with the single-crystal data. However, unlike the single crystal, the increase in resistivity with decreasing temperature is found to be significant, and at 50 K, ρ(polycrystal), in fact, exceeds ρ(single crystal) by three orders of magnitude. It is to be noted that Crawford *et al*, who

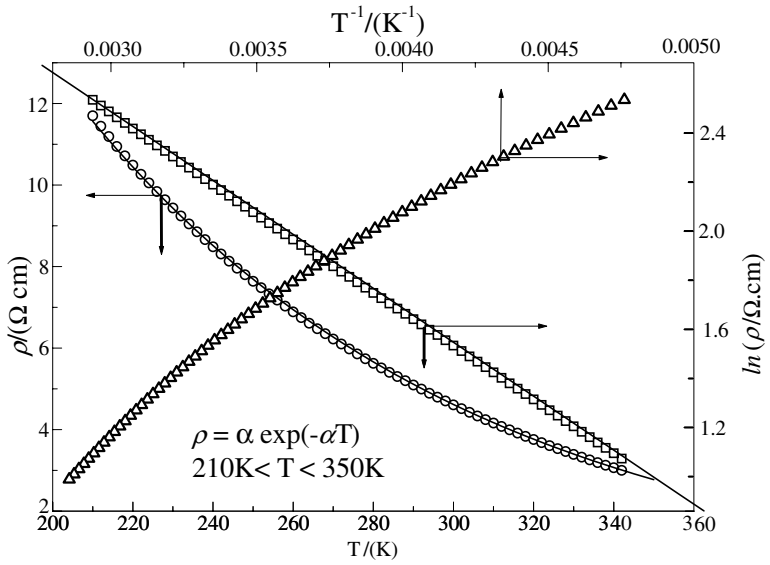

Figure 3. Variation of resistivity with temperature for Sr_2IrO_4 in the temperature range 210 K $<$ T $<$ 350 K. (a) ρ versus T (open circles) and equation (2) (solid line), (b) ln ρ versus T (open squares) and fit (solid line), and (c) ln ρ versus T^{-1} (open triangles).

measured the resistivity of polycrystalline Sr_2IrO_4, reported it to be an insulator [6, 7]. However, both the occurrence of ferromagnetic ordering as well as the transition temperature remain largely unaffected in polycrystalline samples compared to single-crystal samples.

Figure 2 shows various plots of the temperature dependence of resistivity. To get a clear idea of the temperature dependence of resistivity we plotted d[ln(ρ)]/d(T^{-1}) versus T^{-1}. For example, a charge-density-wave (CDW) compound would show a sharp peak in such a plot, as was found in $BaIrO_3$ [1]. It is clear from the figure that no comparable feature exists in the electrical transport of Sr_2IrO_4.

The data in the whole temperature range could not be fitted to a single known model. Three temperature regions were identified in which well defined temperature dependences were observed: a high-temperature region (region I: 350–210 K), in which a logarithmic dependence of temperature ($\rho \propto \exp(-\alpha T)$ or ($\ln \rho \propto -T$) is observed, a middle-temperature region (region II: 190–110 K), in which d[ln(ρ)]/d(T^{-1}) versus T^{-1} is almost flat, indicating an Arrhenius-type behaviour, and a low-temperature region (region III: 80–35 K), in which a three-dimensional variable-range-hopping- (VRH-) type behaviour ($\rho \propto \exp(T_0/T)^{1/4}$ or $\ln \rho \propto T^{-1/4}$) is observed. Below we discuss these behaviours in detail.

Resistivity in the high-temperature region (210–350 K) is shown in figure 3. In this region, the resistivity is found to vary slowly with temperature according to equation (2):

$$\rho(T) = \rho_0 \exp(-\alpha T) \tag{2}$$

where ρ_0 and α are constants obtained by fitting. A temperature range in which a plot of ln ρ versus T data is a straight line was selected and the data were fitted to a straight line to obtain the values of the fitting parameters ρ_0 and α, which were determined to be 98.5(2) Ω cm and 1.0230(8) $\times$ 10^{-2} K^{-1} respectively. It can be seen from the figure that ln ρ versus T is a straight line over a wide temperature range, i.e. 210–350 K. The figure also shows the ρ versus T data, and equation (2) with the fitting parameters (ρ_0 and α) obtained from the

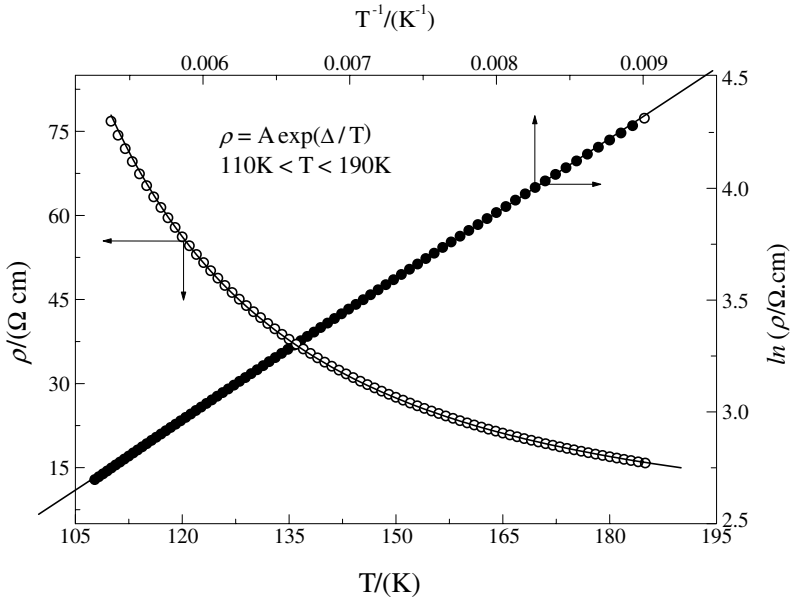

Figure 4. Arrhenius plot and resistivity, $\rho(T)$, data for Sr_2IrO_4 between 110 and 190 K. (a) $\ln \rho$ versus T^{-1} (filled circles) and fitted straight line (solid line), (b) ρ versus T (open circles) and line obtained from equation (3) (solid line).

straight line fitting. For comparison, a plot of $\ln \rho$ versus T^{-1} is also shown in the figure, which is not a straight line, indicating that an Arrhenius-type behaviour is not valid in this temperature range.

Weakly localized two-dimensional metals have been reported to show $\ln \rho \propto -T$ dependence [11, 12]. The weak electronic localization has been reported to take place due to the structural disorder in the material [12, 4].

An accurate structural determination of Sr_2IrO_4 by neutron diffraction on powder samples was carried out by Huang *et al* in 1994 [10]. They measured the powder neutron diffraction at room temperature and at 10 K. They found no structural transition down to 10 K. The structure of Sr_2IrO_4 is made up of corner sharing IrO_6 octahedra stacked along the c-axis of the unit cell [6]. Each layer is 4.14 Å thick and well separated from each other by 2.45 Å. Therefore, the structure is two dimensional in nature. This is also evidenced by the observed lower resistivity within the IrO_6 layer (a-axis) than along the perpendicular direction (c-axis) reported in single crystals [2].

Further, the corner shared IrO_6 octahedra are tilted with respect to each other by 11.36° within the layer at room temperature and by 11.72° at 10 K. Huang *et al* [10] have reported that the disorder arises in the positions of the intra-layer oxygen ions with respect to those of the adjacent layers. About 83% of the oxygen ion positions are generated from those of the previous layers by the operation of the 4_1 axis and about 17% of the oxygen ion positions are generated without any correlation to those in the adjacent layers. Effectively there are two sets of short-range domains in which either of the configurations is present [10].

Figure 4 shows the variation of resistivity with temperature in the middle-temperature range, namely, 110–190 K. A plot of $\ln \rho$ versus T^{-1} is a straight line throughout this temperature range. Moreover, in this range $\mathrm{d}[\ln(\rho)]/\mathrm{d}[T^{-1}]$ versus T^{-1} is almost flat (see figure 2), indicating that an Arrhenius-type behaviour given by equation (3) can be fitted quite

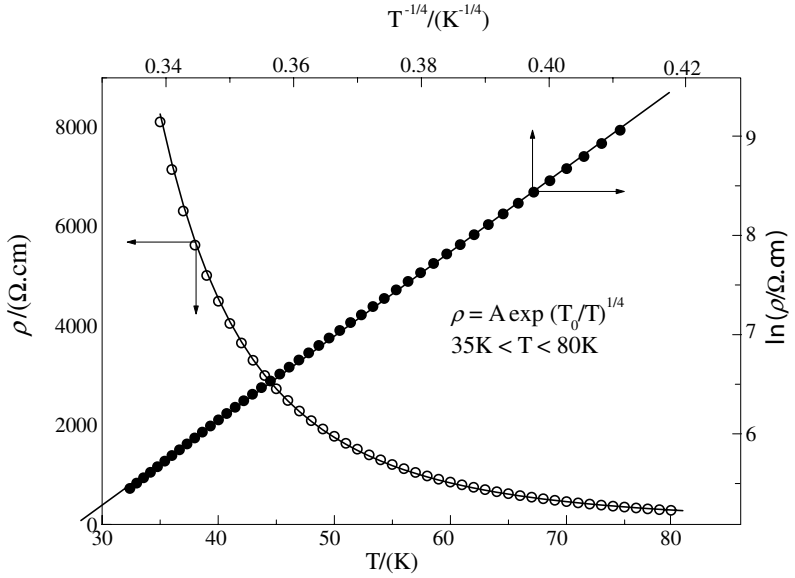

Figure 5. Variation of resistivity with temperature for Sr_2IrO_4 in the low temperature range, 35 K $< T <$ 80 K. (a) ρ versus T (open circles). The solid line on the open circles was obtained by plotting equation (4) with ρ_0 and T_0 obtained from the straight line fit. (b) Variation of ln ρ with $T^{-1/4}$ (filled circles) and a straight line fit to the same (solid line on the filled circles).

reliably.

$$\rho(T) = \rho_0 \exp\left(\frac{\Delta}{k_B T}\right). \tag{3}$$

Therefore, first a straight line was fitted to ln ρ versus T^{-1} data and the values of ρ_0 and Δ were obtained from the intercept and the slope of the straight line respectively. For comparison, a plot of ρ versus T is shown along with the curve obtained from equation (3) using the fitting parameters, $\rho_0 = 1.553(5)$ Ω cm and $\Delta/k_B = 430.7(5)$ K (where k_B is the Boltzmann constant), obtained from the straight-line fit. It can be seen that the two curves match very well.

The gap obtained from the resistivity data is equivalent to 37 meV. Given the fact that room-temperature electrical resistivity of the material is similar to that of a typical semiconductor, such a small value of gap indicates some kind of a pseudogap arising from the localization of electronic states. The situation is comparable to that of $BaIrO_3$ (see [1]). Sr_2IrO_4 shows all the characteristics of $BaIrO_3$ except the charge-density-wave (CDW) transition that coexists with the weak ferromagnetic transition. Recently, Maiti *et al*, through high resolution x-ray photoemission spectroscopy, have shown that there are indeed localized electronic states in $BaIrO_3$ giving rise to a soft gap [5].

Resistivity data in the low temperature region is shown in figure 5 and it can be fitted to a VRH-type behaviour given by equation (4):

$$\rho(T) = \rho_0 \exp\left(\frac{T_0}{T}\right)^{\nu}. \tag{4}$$

A ln ρ versus $T^{-1/4}$ plot in this region was found to be a straight line. Hence the data were fitted to a straight line and the fitting parameters ρ_0 and T_0 were obtained from the intercept and the slope respectively. A curve obtained by plotting equation (4) with $\rho_0 = 1.06(4) \times 10^{-4}$ Ω cm,

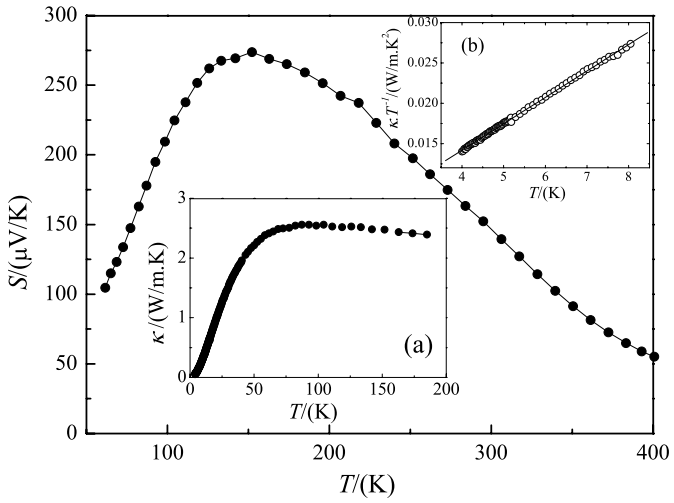

Figure 6. Variation of Seebeck coefficient (S) with temperature for Sr_2IrO_4. Insets (a) and (b) show the temperature dependence of thermal conductivity $\kappa(T)$ and $\kappa \cdot T^{-1}$ versus T respectively.

$T_0 = 3.82(3) \times 10^6$ K (obtained from the straight line fit) and $\nu = 1/4$ was found to match the experimental data very well (see figure 5).

In single crystals, the resistivity along the a-axis was fitted with a variable range hopping (VRH) model, in a rather wide temperature range 190 K $\leqslant T \leqslant$ 300 K. However, the value of the exponent ν was ambiguous [2]. Both $\nu = 1/2$ and $\nu = 1/4$ fitted the observed data reasonably well. It is known that in variable range hopping conductivity the value of ν indicates the dimensionality of the conductor. An n-dimensional conductor is predicted to show a $T^{-1/(n+1)}$ dependence. Hence our data showing a $T^{-1/4}$ dependence indicate a three-dimensional VRH conductivity. We believe that with the decrease in temperature, population of the localized states decreases and hence a three-dimensional VRH conductivity is observed.

3.3. Seebeck coefficient and thermal conductivity

The temperature variations of the Seebeck coefficient $S(T)$ and thermal conductivity $\kappa(T)$ are shown in figure 6 and its inset (a) respectively. $S(T)$ assumes positive values over the whole measured temperature range. The IrO_6 octahedra in Sr_2IrO_4 have a fourfold symmetry along the c-axis with a Ir–O bond-length of 1.98 Å in the ab-plane, while the Ir–O bond-length along the c-axis is 2.05 Å. Therefore, d_{xz} and d_{yz} orbitals are degenerate and have slightly lower energy than the d_{xy} orbital. The five d electrons are distributed as d^2_{xz}, d^2_{yz}, and d^1_{xy}. Thus the d_{xy} orbital accommodates a hole and hence can account for the positive values of thermopower.

The thermopower shows a broad maximum at 150 K where a large value of $S = 270\ \mu V\ K^{-1}$ is reached. It is to be noted that this value is comparable with that observed ($300\ \mu V\ K^{-1}$) in $BaIrO_3$, albeit at a much lower temperature of 70 K [13]. This difference points to an effective depletion of the carrier concentration at a much higher temperature than that in $BaIrO_3$. Other than the broad maximum attained in $S(T)$, the variation of S with T in Sr_2IrO_4 is smooth and no anomalies were observed in the whole measured temperature range (60–400 K), including across the ferromagnetic ordering temperature at $T_c = 250$ K.

The thermal conductivity $\kappa(T)$ of Sr_2IrO_4 (shown in figure 6(b)) exhibits a broad maximum of 2.55 $W\ m^{-1}\ K^{-1}$ at 92 K. A similar maximum in $\kappa(T)$ amounting to

1.2 W m^{-1} K^{-1} was found for $BaIrO_3$ at 30 K [13]. As was the case for $S(T)$, no anomaly has been observed in $\kappa(T)$ of Sr_2IrO_4 across the ferromagnetic transition temperature. As a first approach to interpret the observed behaviour of $\kappa(T)$, we make use of the Wiedemann–Franz law, namely,

$$\kappa_{\mathrm{el}} = \frac{LT}{\rho} \tag{5}$$

relating the electronic thermal conduction to the electrical resistivity through the Lorenz number, $L = 2.45 \times 10^{-8}$ W Ω K^{-2}. This leads to an estimated value at 34 K of $\kappa_{\mathrm{el}} \approx 1 \times 10^{-8}$ W m^{-1} K^{-1}, a value that is entirely negligible compared to the total measured thermal conductivity in Sr_2IrO_4. Therefore, the conduction of heat in Sr_2IrO_4 is predictably ascribed to lattice excitations. In such a case the low-temperature temperature dependence should follow a T^3 dependence through

$$\kappa = \tfrac{1}{3} C_v l \tag{6}$$

in terms of the heat capacity C_v of quasiparticle excitations and $l = v\tau$, the mean free path length. The relaxation rate incorporates, in principle, scattering of phononic excitations from boundaries and from point defects, as well as from Umklapp scattering. In figure 6(b) it is shown that between 4 and 8 K $\kappa(T)$ follows a T^2 dependence, contrary to the above expectation. Since the present polycrystalline samples of Sr_2IrO_4 had to be prepared for bulk thermal transport measurements in the form of pressed and sintered elongated bars, the microscopic grains are acting as effective size constraints on the dominant phononic conduction process, resulting in the much retarded $\kappa(T)$ versus T^2 dependence at low temperatures. The scattering of heat-carrying phononic excitations by electrons can be ignored in Sr_2IrO_4, so that the maximum that is seen in $\kappa(T)$ near 100 K should mainly be ascribed to inelastic scattering processes involving phonon–phonon scattering that inhibits the unabated increase in heat conduction with increased temperature.

However, it is clear that contribution to both Seebeck coefficient and thermal conductivity from the charge carriers is negligible, indicating that the true gap in Sr_2IrO_4 is much larger than the soft gap estimated by electrical resistivity measurements and the density of states near the Fermi level is very small. This scenario is consistent with the specific heat data.

3.4. Specific heat

By careful measurements near the transition temperature, we reported a mean-field anomaly at the transition temperature in polycrystalline $BaIrO_3$ which also shows a weak ferromagnetic transition [13]. Therefore, with the expectation of a similar anomaly, we measured the specific heat on our polycrystalline samples of Sr_2IrO_4. Our studies were made with high density of points at near 250 K. But we could not find any anomalies near the weak ferromagnetic transition. This is not surprising because the transition temperature is 250 K (much higher than that of $BaIrO_3$) where the specific heat is entirely dominated by the phonon contribution.

The specific heat measured between 2 and 290 K is shown in figure 7. The specific heat in the whole temperature range could be well described by a conventional Debye model, according to

$$C_p(T) = 9R \sum_{n=1}^{3} c_n \left(\frac{T}{\theta_{\mathrm{D}_n}}\right)^3 \int_0^{\frac{\theta_{\mathrm{D}_n}}{T}} \frac{x^4 \mathrm{e}^x}{(\mathrm{e}^x - 1)^2}\,\mathrm{d}x \tag{7}$$

where the θ_{D_n} are the fitting parameters. In total, three θ_D were used, one for each of the ions, namely Sr^{2+}, Ir^{4+}, and O^{2-}. The index c_n indicates number of ions: 2, 1, and 4 for Sr^{2+}, Ir^{4+}, and O^{2-} respectively, according to the formula unit. The solid line in figure 7 shows the fitted

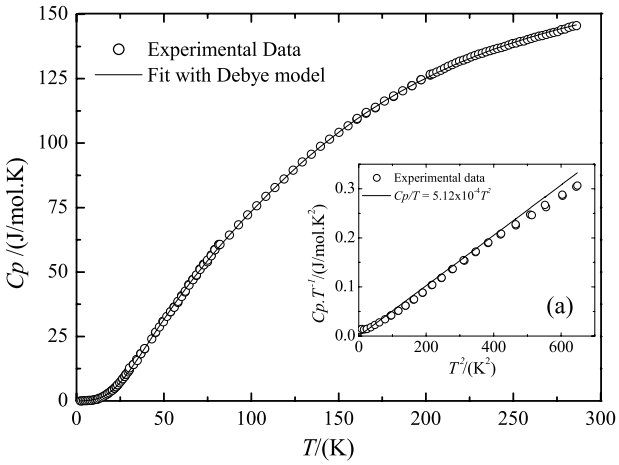

Figure 7. Specific heat (C_p) data of Sr_2IrO_4 as a function of temperature T: experimental (open circles) and fitted data (solid line). The inset shows the C_p/T versus T^2 plot for experimental data (circles). The solid line in the inset corresponds to $C_p^{\text{phonon}}/T = \beta T^2$ with β obtained from equation (8) (see text).

data with $\theta_D = 279$, 184, and 725 K respectively for Sr^{2+}, Ir^{4+}, and O^{2-}. A C_p/T versus T^2 plot (see figure 7(a)) yields an almost straight line with a negligible intercept, over a wide temperature range 5–25 K, showing that also at these temperatures C_p is completely dominated by phonons. This is not surprising, not only because there is no anomaly at T_c but also because the contribution of the magnetic excitations to the specific heat are expected to be extremely small below 25 K due to the high Curie temperature. On the other hand the huge increase of the resistivity towards low temperatures indicates a complete depletion of charge carriers as shown by the observed VRH-type behaviour in the resistivity. Then their contribution to the specific heat is also expected to vanish. The straight line in figure 7(a) corresponds to $C_p^{\text{phonon}} = \beta T^3$ with β calculated using equation (8)

$$\beta = \frac{12\pi^4 R}{5} \sum_{n=1}^{3} c_n \left(\frac{1}{\theta_{D_n}} \right)^3 \tag{8}$$

with the θ_{D_n} obtained from the previous Debye fit in the whole temperature range 2 K $< T <$ 285 K. Since the total specific heat is very close to C_p^{phonon} in the whole temperature range, the data for $T < 25$ K show that if there is a γT contribution of the electrons at all then the Sommerfeld coefficient γ is very small. In fact, when fitted to the equation $C_p/T = \gamma T + \beta T^2$, the data in the temperature range 7 K $< T <$ 25 K give an upper limit of 2 mJ K^{-2} mol^{-1} for γ which is in excellent agreement with the value reported for polycrystalline samples in a low temperature C_p measurement [8]. This low γ value points to a very small density of electronic states at the Fermi level consistent with the depleted localized states at low temperatures. Unfortunately, a small additional contribution to C_p/T at temperatures below 7 K prevents a more precise determination. The origin of the additional term is not clear, but it is conceivable that boundary scattering of heat-carrying phonons, together with the phononic mean-free path (equation (5)) becoming comparable in length to the particle size in our sintered sample, might be responsible for this low temperature contribution. This is consistent with the observed higher resistivities in our polycrystalline samples than the averaged single-crystal resistivity.

4. Conclusion

We have prepared polycrystalline Sr_2IrO_4 samples and investigated their magnetic, transport, and thermodynamic properties. The magnetic behaviour of our polycrystalline samples is very similar to that reported for single crystals. We confirm a Curie–Weiss susceptibility with a rather small effective moment $\mu_{\rm eff} = 0.33\ \mu_{\rm B}$/Ir at high temperature, and weak ferromagnetic order below $T_{\rm c} = 250$ K, with a small saturated moment $\mu_{\rm s} = 0.06\mu_{\rm B}$/Ir. In contrast, the semiconducting-like behaviour of the resistivity is much more pronounced in our polycrystalline samples than in the single crystals, ρ (50 K) being three orders of magnitude larger than ρ (300 K). The temperature dependence of resistivity points to a gradual transition from weakly localized two-dimensional conductivity at high temperatures to a small gapped system at middle temperatures to three-dimensional VRH-type conductivity at low temperatures.

Thermal activation of charge carriers across an energy gap is also evidenced by a large Seebeck coefficient showing a broad maximum of 270 μV K^{-1} at 150 K, while the specific heat is completely dominated by the phonon contribution in the temperature range 5 K $< T <$ 300 K. This does not allow for a determination of magnetic or electronic contributions.

No anomalies are visible in $\rho(T)$, $C_p(T)$ or $S(T)$ at $T_{\rm c}$. The absence of a visible anomaly in $C_p(T)$ is not surprising in view of the small value of the ordered moment, which usually goes along with a small value of the entropy change associated with the ordering process. The absence of any anomaly in the electronic transport is more surprising, since small values of the effective moment point to an itinerant character of the d electrons. A plausible scenario arising from the temperature-dependent resistivity of our polycrystalline samples is something like a system in which spin polarization takes place within the sharply peaked DOS and localized states lift the Fermi level away from the band edge, giving rise to the low density of states observed in various physical properties. Thus the electronic transport becomes insensitive to the magnetic ordering that takes place within the adjacent spin-polarized bands.

The interesting semiconducting system Sr_2IrO_4 is clearly inviting further in-depth investigations involving magnetic, transport as well as local probes in order to elucidate the physical mechanisms at work in this system at the confluence of activated transport behaviour and delocalized magnetism.

Acknowledgment

AMS gratefully acknowledges the hospitality of the Max Planck Institute for Chemical Physics of Solids, Dresden.

References

[1] Cao G, Crow J E, Guertin R P, Henning P F, Homes C C, Strongin M, Basov D N and Lochner E 2000 *Solid State Commun.* **113** 657–62
[2] Cao G, Bolivar J, McCall S, Crow J E and Guertin R P 1998 *Phys. Rev.* B **57** R11039–42
[3] Cao G, Xin Y, Alexander C S, Crow J E, Schlottmann P, Crawford M K, Harlow R L and Marshall W 2002 *Phys. Rev.* B **66** 214412
[4] Whangbo M-H and Koo H-J 2001 *Solid State Commun.* **118** 491–5
[5] Maiti K, Singh R S, Medicherla V R R, Rayaprol S and Sampathkumaran E V 2005 *Phys. Rev. Lett.* **95** 016404
[6] Crawford M K, Subramanian M A, Harlow R L, Fernandez-Baca J A, Wang Z R and Johnston D C 1994 *Phys. Rev.* B **49** 9198–201
[7] Subramanian M A, Crawford M K, Harlow R L, Ami T, Fernandez-Baca J A, Wang Z R and Johnston D C 1994 *Physica* C **235–240** 743–4

[8] Carter S A, Batlog B, Cava R J, Krajewski J J, Peck W F Jr and Rupp L W Jr 1995 *Phys. Rev.* B **51** 17184–7
[9] Itoh M, Shimura T, Inaguma Y and Morii Y 1995 *J. Solid State Chem.* **118** 206–9
[10] Huang Q, Soubeyroux J L, Chmaissem O, Natali Sora I, Santoro A, Cava R J, Krajewski J J and Peck W F Jr 1994 *J. Solid State Chem.* **112** 355–61
[11] Litteer J B, Chen B H, Fettinger J C, Eichhorn B W, Ju H L and Greene R L 2000 *Inorg. Chem.* **39** 458–62
[12] Gourdon O, Evain M, Jobic S, Brec R, Koo H-J, Whangbo M-H, Corraze B and Chauvet O 2001 *Inorg. Chem.* **40** 2898–904
[13] Kini N S, Bentien A, Ramakrishnan S and Geibel C 2005 *Physica* B **359–361** 1264–6